Journal of Hazardous Materials 168 (2009) 121–128

Contents lists available at ScienceDirect

Journal of Hazardous Materials

journal homepage: www.elsevier.com/locate/jhazmat

Effects of particle size and acid addition on the remediation of chromite ore processing residue using ferrous sulfate

Santhi Chandra Jagupilla[a], Deok Hyun Moon[a], Mahmoud Wazne[a,*], Christos Christodoulatos[a], Min Gyu Kim[b]

[a] W.M. Keck Geoenvironmental Laboratory, Center for Environmental Systems, Stevens Institute of Technology, Hoboken, NJ 07030, USA
[b] Beamline Research Division, Pohang Accelerator Laboratory, Pohang University of Science and Technology, Pohang 790-784, South Korea

ARTICLE INFO

Article history:
Received 13 June 2008
Received in revised form 6 December 2008
Accepted 5 February 2009
Available online 12 February 2009

Keywords:
Chromite ore processing residue (COPR)
Ferrous sulfate
Toxicity characteristic leaching procedure (TCLP)
X-ray absorption near edge structure (XANES)
X-ray powder diffraction (XRPD)

ABSTRACT

A bench-scale treatability study was conducted to assess the effects of particle size and acid addition on the remediation of chromite ore processing residue (COPR) using ferrous sulfate. The remediation scheme entailed the chemical reduction of hexavalent chromium [Cr(VI)] and the mitigation of swell potential. Leaching tests and the EQ3/6 geochemical model were used to estimate the acid dosage required to destabilize Cr(VI)-bearing and swell-causing minerals. The model predicted greater acid dosage than that estimated from the batch leaching tests. This indicated that mass transfer limitation may be playing a significant role in impeding the dissolution of COPR minerals following acid addition and hence hindering the remediation of COPR. Cr(VI) concentrations determined by alkaline digestion for the treated samples were less than the current NJDEP standard. However, Cr(VI) concentrations measured by X-ray absorption near edge structure (XANES) were greater than those measured by alkaline digestion. Greater Cr(VI) percentages were reduced for acid pretreated and also for smaller particle size COPR samples. Upon treatment, brownmillerite content was greatly reduced for the acid pretreated samples. Conversely, ettringite, a swell-causing mineral, was not observed in the treated COPR.

1. Introduction

Chromite ore processing residue (COPR) is the solid residue left after the extraction of hexavalent chromium [Cr(VI)] from chromite ore using the high lime process. The extraction process involves mixing the chromite ore with lime and soda ash at approximately 1200 °C to oxidize chromium (Cr) from trivalent to hexavalent state and to sequester impurities. The detailed description of the extraction process was described by numerous researchers [1–4]. Millions of metric tons of COPR had been deposited at many urban areas in the USA, UK and some other places around the world [5–8]. COPR is highly alkaline ($pH > 12$) and it contains unreacted chromite and unextracted chromate. The total Cr concentrations in COPR are up to 5%, including hexavalent chromium [Cr(VI)] concentration up to 2% on dry weight basis [9–11]. Two problems are observed at COPR deposition sites in the USA: the first problem is leaching of chromate solution and the second one is heaving and uncontrolled expansion [7]. Hence, COPR has become a major geoenvironmental and geotechnical hazard in many urban areas. COPR hazards stems from its mineralogical composition. It is comprised mainly of brownmillerite ($Ca_4Fe_2Al_2O_{10}$), periclase (MgO), quicklime (CaO) and their hydration products such as hydrogarnets ($Ca_3Al_2(OH)_{12}$), portlandite ($Ca(OH)_2$), and brucite ($Mg(OH)_2$.

The COPR minerals can be grouped into two classes; fast reactants and slow reactants. Fast reactants are mainly hydrates and carbonates, which react within minutes, whereas, slow reactants are mainly brownmillerite and periclase, which may take up to months or years for the reactions to be complete. Tamas and Vertes [12] reported complete hydration of synthetic brownmillerite in less than 2 weeks. However, brownmillerite at a New Jersey site is still present some 80 years after its deposition [1,4,6–11]. The hydration of brownmillerite in COPR appears to be kinetically inhibited. The slow hydration of brownmillerite results in the delayed release of alkalinity and alumina, which may prove detrimental to the remediation process due to the potential for future swell of the treated COPR material. Moreover, Cr(VI)-bearing minerals can be embedded in brownmillerite as reported by Kremser et al. [13] and Hillier et al. [14]. Kremser et al. [13] presented an electron probe microscope image of a COPR nodule where a Cr(VI)-bearing mineral was embedded within the brownmillerite mineral.

In the environment, chromium exists in two stable oxidation states, trivalent chromium [Cr(III)] and Cr(VI). Cr(VI) is carcinogenic and mobile in alkaline conditions, while Cr(III) is a micronutrient and immobile at $pH > 5$ [4,15]. Hence, most of the applied

---

* Corresponding author. Tel.: +1 201 216 8993 fax: +1 201 216 8212.
E-mail address: mwazne@stevens.edu (M. Wazne).

0304-3894/$ – see front matter © 2009 Elsevier B.V. All rights reserved.
doi:10.1016/j.jhazmat.2009.02.012

remediation techniques involved the chemical reduction of Cr(VI) to Cr(III) followed by precipitation to Cr(III) hydroxides. Some of the more effective reductants are ferrous iron [Fe(II)] [7,10,11,16,17], calcium polysulfide [9,10,18,19], and sodium dithionite [20]. This paper deals with Fe(II) in the form of ferrous sulfate heptahydrate even though all prior attempts to remediate COPR in NJ using Fe(II) sources have failed to achieve satisfactory results.

The reduction of Cr(VI) by Fe(II) is based on the following reaction [7].

$$3Fe^{2+} + CrO_4{}^{2-} + 8H_2O \rightarrow 4Fe_{0.75}Cr_{0.25}(OH)_3 + 4H^+ \qquad (1)$$

The use of Fe(II) salt in its sulfate form is advantageous in treating COPR. Geelhoed et al. [17] reported a large increase in Cr(VI) leachability caused by sulfate exchange with chromate anions in Cr(VI)-bearing minerals such as hydrocalumites. Another advantage for using Fe(II) is that it imparts acidity due to the release of H^+ ions as shown in Eq. (1). On the other hand, infusion of sulfates into COPR matrices can create heave problems. Ettringite, a heaving culprit in COPR and cement chemistry, was formed at pH greater than 9 in the presence of sulfate in COPR treated samples [7,11].

A pilot scale study which was conducted at a site in New Jersey, USA using ferrous sulfate heptahydrate at 5 and 8 times the stoichiometric requirement (38% and 51%, respectively) failed to achieve satisfactory results after a curing period of 240 days [7,11]. Dermatas et al. [7] reported on the use of three types of mixers-pugmill, horizontal rotary mixing and vertical auger. The Cr(VI) concentrations, as measured by alkaline digestion, were less than 240 mg/kg immediately after mixing but increased over time. Cr(VI) concentrations were also measured by X-ray absorption near edge structure (XANES) and the lowest Cr(VI) concentration reported was 588 mg/kg for vertical auger mixing with a ferrous sulfate heptahydrate dosage of 38% (w/w) after 240 days curing time. The reasons for failure are attributed to the slow leaching of Cr(VI) from the COPR nodules due to mass transfer limitations and the scavenging of the Fe(II) reductant by oxygen during treatment and curing. Therefore any treatment schemes should mitigate mass transfer limitations by measures such as reduction of COPR particle size, destabilization of Cr(VI)-bearing minerals, and effective mixing.

The effect of particle size on the treatment results was shown in a recent study by Moon et al. [11]. Moon et al. [11] reported on long-term treatment issues associated with COPR for the same pilot study. The cited study compared Cr(VI) reduction in two types of COPR (B1B2 and C) using ferrous sulfate heptahydrate. The particle size of Type C COPR is smaller than the particle size of type B1B2. Greater Cr(VI) reduction rates were observed in Type C COPR, suggesting that particle size reduction prior to the addition of the reductant may improve the effectiveness of the treatment. Moreover, reduction of particle size exposes more surface area thus resulting in the release of more Cr(VI) that are embedded in the COPR minerals. The released Cr(VI) ions are more readily available for chemical reaction with the ferrous ions than the embedded ones.

On the other hand, Wazne et al. [4] investigated the stability regions of Cr(VI)-bearing and swell-causing minerals. The Cr(VI)-bearing minerals identified in COPR were calcium aluminum oxide chromium hydrates (CACs) (monochromate or Cr(VI)-hydrocalumite), hydrotalcites and hydrogarnets [4,21]. The solubility of Cr(VI) was found controlled by Cr(VI)-ettringite and Cr(VI)-hydrocalumite minerals at a pH range of 10.5–11.5 and pH greater than 11.5, respectively. According to the study, imparting acidity into COPR destabilizes Cr(VI)-bearing minerals and makes Cr(VI) available for reaction with Fe(II). The leaching studies as reported by Wazne et al. [4] and Tinjum et al. [22] indicated a measured increase in Cr(VI) leachability at pH values between 5 and 10, where the maximum amount of Cr(VI) was leached in the pH range of 7.6–8.1, respectively. Also, at pH less than 9 the formation of the swell-causing mineral, ettringite, appears to be inhibited. This implies that the maintenance of COPR pH below 9 favors the dissolution of Cr(VI)-bearing and swell-causing minerals. Moreover, the alkaline pH of COPR favors the precipitation of Fe(II) as ferrous hydroxides or carbonates and the oxidation of Fe(II) to Fe(III) by oxygen [7,17]. Therefore, COPR treatment should be attempted with enough acidity to bring the pH to less than 9.

Moon et al. [19] had published the effect of particle size and pH on the remediation of COPR using calcium polysulfide (CaS_5) as the reductant. The results of the CaS_5 showed that the treatment was not very effective even at pH less than 9. The treatment results were not satisfactory with respect to residual Cr(VI) and ettringite formation. It was suspected that the acid dosage needed to bring the treatment pH values to less than 9, as estimated empirically from the ANC tests (2 months mixing time) was not sufficient to keep the pH at target values. Therefore an alternative approach was necessary to estimate this acid dosage, which led us to conduct an extensive geochemical modeling work to estimate the amount of acid needed to reach the target pH, without any rebound in pH upon mixing or long term treatment.

In this study, ferrous sulfate heptahydrate with a dosage of 25% (w/w) was used for the treatment. The COPR particle size ranged from 0.150 to 0.010 mm, whereas, the amount of acid dosage needed to maintain pH less than 9 was estimated from leaching tests and EQ3/6 geochemical modeling. The toxicity characteristic leaching procedure (TCLP) Cr concentration for treated samples was measured and compared with the universal treatment standards (UTS) of 0.6 mg/L. Alkaline digestion and X-ray absorption near edge structure (XANES), a non-destructive technique, were used to measure the concentration of Cr(VI) in all COPR samples. Qualitative and quantitative X-ray powder diffraction (XRPD) analyses were conducted for the untreated and treated COPR samples to understand the mineralogical transformations and to assess the treatment results.

2. Materials and methods

2.1. Materials

2.1.1. COPR samples

The COPR samples used in this study were collected during a major sampling event from study area 7 (SA7) in Jersey City, New Jersey, USA. The samples were collected from two stratigraphic layers, B1 and B2, extending from the ground surface to 4–5 m below ground surface (bgs). The detailed description of the physical characterization of the COPR layers was presented in Dermatas et al. [6] and Wazne et al. [9]. The water table fluctuates in the B2 zone. A homogenized B1B2 sample was prepared by mixing equal amounts of COPR from zones B1 and B2. After homogenization, the sample was air dried and pulverized to achieve lower particle sizes. Four different particle sizes were used in this study, which consisted of COPR material passing through sieves-mesh 100 (<0.150 mm), mesh 200 (<0.075 mm), mesh 400 (<0.038 mm) and micronized COPR (<0.010 mm). The micronized COPR was obtained by grinding air dried COPR with cyclohexane in a McCrone micronizing mill (Westmont, IL) and then air drying the mixture. It is worth noting here that, when the COPR sample was passed through a particular sieve to achieve the required particle size, the entire quantity of COPR sample was made to pass through the sieve to avoid any fractionation.

2.1.2. Reagents

Ferrous sulfate heptahydrate ($FeSO_4 \cdot 7H_2O$), potassium chromate (K_2CrO_4), chromium nitrate nonahydrate [$Cr(NO_3)_3 \cdot 9H_2O$], concentrated sulfuric acid, concentrated hydrochloric acid, sodium

Table 1
Treatment conditions for COPR.

Sample ID	Particle size (mm)	Reductant dosage % (w/w)[a]	Acid pretreated (yes/no)
COPR1-150-NA	≤0.150	25	No
COPR2-150-A	≤0.150	25	Yes
COPR3-075-NA	≤0.075	25	No
COPR4-075-A	≤0.075	25	Yes
COPR5-038-NA	≤0.038	25	No
COPR6-038-A	≤0.038	25	Yes
COPR7-010-NA	≤0.010	25	No
COPR8-010-A	≤0.010	25	Yes

[a] Percent of dry weight of COPR.

hydroxide, sodium carbonate, and cyclohexane were certified ACS grade and were obtained from Fisher Scientific (Suwanee, GA).

2.2. *Experimental design and methods*

2.2.1. *Design*

The experimental design to investigate the effects of particle size and acid dosage is presented in Table 1. The dosage of ferrous sulfate heptahydrate is the same for all treatment conditions, at approximately twice the Cr(VI) stoichiometric requirement and is equivalent to 25% (w/w). At each particle size, the samples were acid treated prior to the addition of the reductant. The acid dosage was diluted into the required water quantity and mixed with COPR before the addition of the ferrous sulfate dosage. Control duplicate experiments were conducted at each particle size with no acid pretreatment. The samples were mixed rigorously with the ferrous sulfate and sulfuric acid (when applicable) for 1 h at a liquid to solid ratio of 10. After mixing, the samples were filtered and the COPR residue was subjected to alkaline digestion, TCLP, XANES and XRPD analyses.

2.2.2. *Leaching tests*

The amount of mineral acid needed to destabilize the Cr-bearing minerals and the swell-causing minerals as determined from ANC tests [23] have been previously reported by Wazne et al. [10]. A COPR sample of particle size less than 0.150 mm was mixed with different equivalents of acid and water at a liquid to solid ratio of 20, to achieve pH values ranging from 1 to 12. The samples were prepared in duplicates and mixed in an end-over-end mixer for 1 week and 2 months, before the pH was measured. However, the required acid dosage was also obtained through geochemical modeling. The geochemical modeling code, EQ3/6, developed at Lawrence Livermore National Laboratory (LLNL) was used to simulate COPR–water interactions [24,25]. The LLNL database is one of the most extensive resources available and contains many minerals that are pertinent to the COPR mineral system. The database was also supplemented by COPR phases reported in the literature [3,4]. The input used in the model was the percent weight of the mineral phases as obtained by Rietveld quantification. The amorphous content was assumed to consist of goethite during the modeling runs. Typically, the major sources of amorphous content are silicon and iron oxides; the measured concentrations of Si and Fe in the COPR samples were approximately 1.98% and 11.8%, respectively [19]. The small amount of Si can sequester in quartz, albite, and hydroadratite, whereas there is no clear sink for the large iron content in the COPR minerals. Amorphous content could not be used as input in the model calculations so goethite was used as a surrogate for the iron oxide–hydroxide. Iron in COPR is generated due to the hydration of brownmillerite to hydrogarnet (non-iron phase) and iron oxide–hydroxide. However, it is widely accepted in the literature that hematite is abundant in ancient deposits whereas goethite is abundant in younger deposits [26]; therefore goethite was used as a surrogate for the amorphous content. COPR was titrated with acid during the model simulation and all reactions were assumed to occur instantaneously.

2.2.3. *Physicochemical analyses*

pH values for all COPR samples were measured as per ASTM D4972-01 [27]. The total concentration of chromium in the treated samples was measured using US Environmental Protection Agency (USEPA) Method 3051A, microwave assisted acid digestion [28] and USEPA Method 6010C, Inductive Coupled Plasma-Atomic Emission Spectroscopy (ICP-AES) [29]. For quality control purposes, Montana standard soil was used for the acid digestion process. The Cr ICP standard was used for the calibration of ICP-AES and quality control blank and spikes were measured for every 10 samples per batch. The concentration of Cr(VI) in COPR was measured using the USEPA Method 3060A, alkaline digestion method [30]. A representative sample of 2.5 g of the COPR material was digested in phosphate buffered alkaline digestion solution (0.28 M Na_2CO_3/0.5 M NaOH) at 90–95 °C for about 60–65 min. 100 mg of Mg^{2+} in the form of magnesium chloride was also added to the digestion solution to suppress the oxidation of Cr(III). The digested solution was allowed to cool to room temperature. The solution was then filtered using Millipore Nylon-66, 0.45 μm membrane filters. The Cr(VI) concentration in the filtrate was measured using the USEPA Method 7196A, colorimetric analyses [31]. In colorimetric analyses, diphenylcarbazide reagent was used to react with Cr(VI) in acid solution, which produces a red-violet product. The absorbance was measured at 540 nm in the spectrophotometer, to measure aqueous Cr(VI) concentration. Turbidity blanks were incorporated into the analysis procedure. Cr(VI) solution in the form of K_2CrO_4 was used for the calibration of spectrophotometer. Blank and spike recoveries were conducted to check the accuracy of the method. The toxicity characteristic leaching procedure (TCLP) of Cr was conducted as per USEPA Method 1311 [32]. Briefly, 3 g of sample was mixed with 60 mL of TCLP extraction fluid, and tumbled for 18 h at 30 ± 2 rpm. The post tumbling pH of the sample was recorded and the leachate was filtrated through a polycarbonate filter with an effective pore size of 0.45 μm. The concentration of Cr in the filtrate was measured using ICP-AES.

2.2.4. *Mineralogical analyses*

XRPD technique was used to assess the mineralogical composition of the untreated and treated COPR samples. XRPD sample preparation included pulverization of a 2 g homogenized COPR sample with 7 mL cyclohexane in the McCrone micronizing mill for 5 min. The resulting slurry was air dried and then mixed with corundum (α-Al_2O_3, Sawyer, Lot No. C04-AO-41) on an 80:20 weight basis and was subjected to XRPD. Corundum was used to determine the amorphous content in the COPR samples. Step-scanned XRPD data was collected by the Rigaku DXR-3000 computer-automated diffractometer using Bragg-Brentano geometry. The diffractometry was conducted at 40 kV and 40 mA using a diffracted beam graphite-monochromator with Cu radiation. The data was collected in the 2θ range of 5° to 65° with a step size of 0.02° per 3 s. The qualitative and quantitative analyses of the XRPD patterns were performed using the Jade software [33], version 7.5 and the Whole Pattern Fitting function of Jade, which is based on the Rietveld method [34]. The reference databases for powder diffraction and crystal structure data were the International Center for Diffraction Data database [35] and the Inorganic Crystal Structure Database [36], respectively.

2.2.5. *X-ray absorption near edge structure (XANES)*

XANES, being a non-destructive technique, was used to determine the Cr(VI) concentrations in the treated samples. XANES patterns were collected at the Pohang Accelerator Laboratory (PAL),

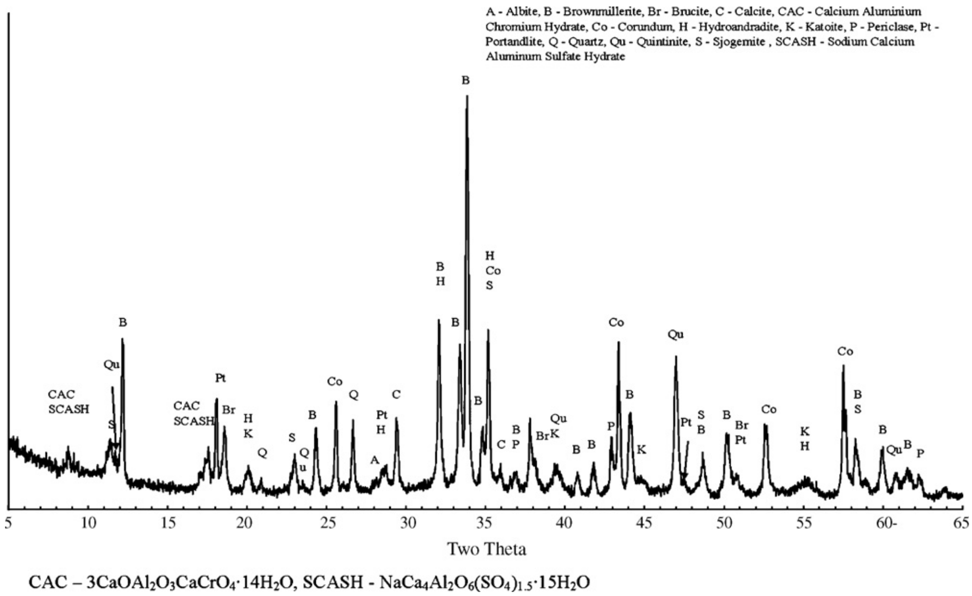

Fig. 1. XRPD pattern for untreated COPR.

South Korea using a BL7C1 (Electrochemistry) beamline in a storage ring of 2.5 GeV with a ring current of 130–185 mA. A Si(1 1 1) double crystal monochromator was used and high order harmonic contamination was eliminated by detuning the monochromator to reduce the incident X-ray intensity by approximately 30%. All spectroscopic data were collected in the fluorescence mode using pure N_2 gas-filled ionization chambers as gas detectors. Energy calibration was simultaneously performed for each measurement using a reference Cr foil placed in front of the third ion chamber, and assigning the first inflection point to 5989 eV. The chromium compounds, potassium chromate (K_2CrO_4) and chromium nitrate nonahydrate [$Cr(NO_3)_3{\cdot}9H_2O$] were used as the standard reference for Cr(VI) and Cr(III), respectively. The ATHENA program in the IFEFFIT computer package was used for the quantitative XANES analyses [37].

3. Results and discussion

3.1. Initial characterization

The pH of the untreated COPR samples varied from 12.03 to 12.25, with an average value of 12.14. The concentrations of Cr(VI) as measured using alkaline digestion [30] and colorimetric analysis [31] for the untreated COPR for the four different particle sizes ranged from 4575 to 6530 mg/kg. Specifically, Cr(VI) concentrations were 4575, 4974, 6478 and 6530 mg/kg for samples with particle sizes less than 4.75 mm, less than 0.15 mm, less than 0.075 mm and less than 0.01 mm, respectively. This indicated that greater Cr(VI) quantities were extracted as the particle size of the COPR samples was reduced. However, Cr(VI) concentration was measured at 7588 mg/kg by Wazne et al. [9] and Moon et al. [11] using XANES.

The XRPD pattern of the untreated COPR is presented in Fig. 1 and the mineralogical quantification is presented in Table 2. Brownmillerite was the major phase observed in the untreated COPR measured at approximately 31%. However, brownmillerite is not stable thermodynamically under aqueous conditions and should have hydrated to hydrogarnets [$Ca_3Al_2(OH)_{12}$], portlandite [$Ca(OH)_2$] and hematite (Fe_2O_3) according to the following reaction:

$$Ca_4Fe_2Al_2O_{10} + 7H_2O \rightarrow Ca(OH)_2 + Fe_2O_3 + Ca_3Al_2(OH)_{12} \qquad (2)$$

Cr(VI)-hydrocalumite (calcium aluminum chromium oxide hydrate, CAC, $3CaOAl_2O_3CaCrO_4{\cdot}14H_2O$) was the only Cr(VI) phase identified in the XRPD pattern. The quantity of Cr(VI)-hydrocalumite identified in the COPR sample was measured at 1.28%, which corresponds to a Cr(VI) concentration of approximately 750 mg/kg. However, this is about 10% of the total Cr(VI) concentration in the untreated COPR sample. The remaining Cr(VI) could be present in other mineral phases such as hydrogarnet and hydrotalcites [4,21]. Numerous minor phases were also detected as shown in Table 2. Calcite was measured at approximately 6%. Calcite could have formed upon carbonation of COPR after deposition. Silicate phases such as hydroandradite, albite and quartz were measured at approximately 5%, 3% and 2%, respectively. Silicon could have originated from the chromite ore or it could have come from contact of COPR with indigenous soils. Brucite and periclase were measured at approximately 4% and 3%, respectively. These two phases serve as sinks for magnesium; however, brucite is the hydration byproduct of periclase. The rest of magnesium could also be present in hydrotalcite phases such as quintinite, sjogrenite, which are present at approximately 2% each. It is worth noting that periclase is not stable under environmental conditions and should hydrate to brucite and hydrotalcites. Finally, the amorphous

Table 2
Quantitative Results of untreated COPR.

Mineral name	Untreated COPR (%)
Calcium aluminum oxide chromium hydrate (CAC), $3CaOAl_2O_3CaCrO_4{\cdot}14H_2O$	1.28
Sodium calcium aluminum sulfate hydrate, $NaCa_4Al_2O_6(SO_4)_{1.5}{\cdot}15H_2O$	2.49
Brownmillerite, $Ca_2(Al, Fe^{3+})_2O_5$	31.20
Brucite, $Mg(OH)_2$	3.83
Calcite, $CaCO_3$	5.78
Hydroandradite, $Ca_3Fe_2(SiO_4(OH)_4)_3$	4.71
Katoite, $Ca_3Al_2(OH)_{12}$	3.83
Periclase, MgO	2.56
Portlandite, $Ca(OH)_2$	1.88
Quartz, SiO_2	2.15
Quintinite, $Mg_4Al_2(OH)_{12}(CO_3){\cdot}3H_2O$	1.85
Sjogrenite, $Mg_6Fe^{2+}{}_2CO_3(OH)_{16}{\cdot}4H_2O$	2.22
Albite, $NaAlSi_3O_8$	3.43
Amorphous	32.75
Total	99.97

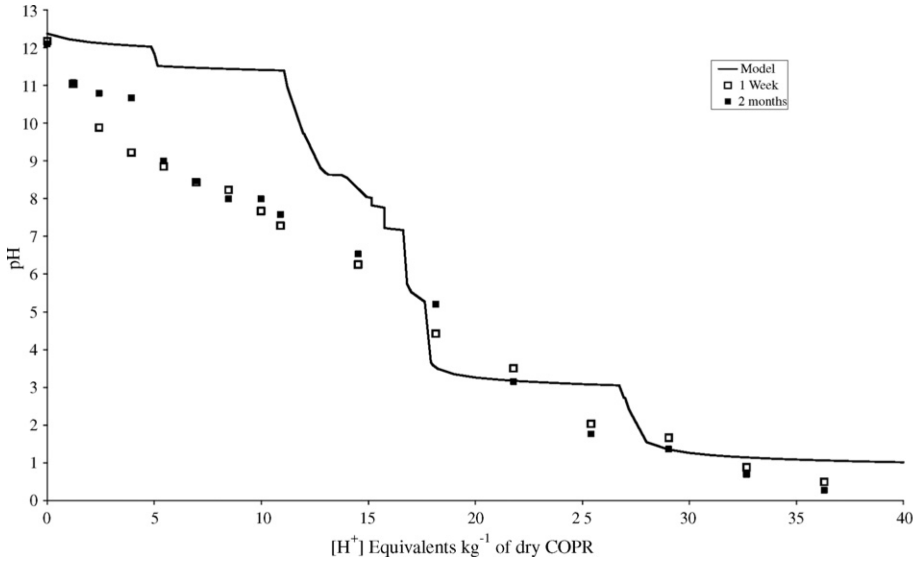

Fig. 2. ANC and model results for COPR sample.

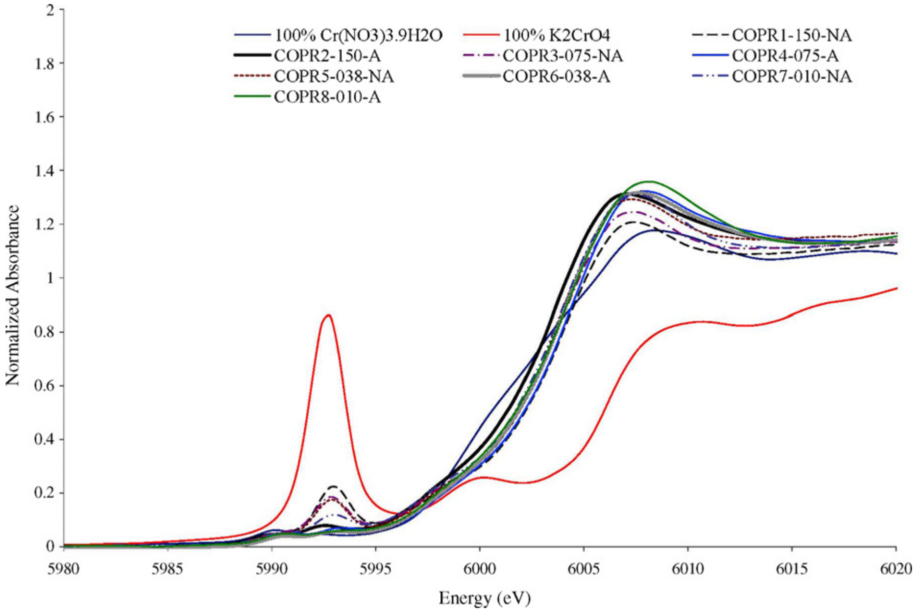

Fig. 3. Chromium K-edge XANES patterns for treated COPR.

content was determined to be approximately 33% using corundum as an internal standard.

3.2. Leaching tests

The pH results from the ANC tests after a mixing time of 1 week and 2 months are shown in Fig. 2 as reported in Wazne et al. [10]. The pH values are virtually similar at all the acid dosages except at 4 eq [H$^+$]/kg. This could be due to the slow hydration of the COPR minerals. The pH results obtained from the EQ3/6 model are also presented in Fig. 2. The model predicted a higher acid dosage than the ANC tests at a pH greater than 6. This may indicate that the hydration of COPR minerals is slow and also that the system had not reached equilibrium even after 2 months. Though the ANC tests indicate that an acid dosage of 5.5 eq [H$^+$]/kg is needed to achieve a pH below 9, the model predicted an acid dosage of 13 eq [H$^+$]/kg to attain the same pH value. As the addition of ferrous sulfate at 25% provides 1.8 eq [H$^+$]/kg, an additional 11.2 eq [H$^+$]/kg was needed in the form of added acid to attain the required dosage. The acid dosage used was approximately 0.31 L concentrated sulfuric acid per 1 kg of dry weight COPR.

Table 3
Results of ferrous sulfate treated COPR.

Sample ID	Treatment pH	Cr(VI)[a] (mg/kg)	TCLP Cr (mg/L)	TCLP pH
COPR1-150-NA	8.59	<2	10.89	8.37
COPR2-150-A	7.25	<2	2.43	7.49
COPR3-075-NA	8.54	<2	10.65	8.51
COPR4-075-A	7.75	<2	1.52	6.75
COPR5-038-NA	8.54	<2	11.33	7.95
COPR6-038-A	7.77	<2	1.08	6.82
COPR7-010-NA	8.55	<2	7.49	7.58
COPR8-010-A	6.80	<2	0.55	6.96

Note: Method detection limit (MDL)—2 mg/kg.

[a] Cr(VI) was measured using alkaline digestion and colorimetry.

Table 4
XANES results for treated COPR samples.

Sample ID	Total Cr (mg/kg)	Cr(VI) (%)	Cr(III) (%)	Cr(VI) (mg/kg)	Cr(III) (mg/kg)	% Reduction of Cr(VI)
COPR1-150-NA	27,473	21	79	5769	21,704	23.97
COPR2-150-A	26,435	4	96	1057	25,378	86.06
COPR3-075-NA	27,632	16	84	4421	23,211	41.74
COPR4-075-A	27,219	2	98	544	26,675	92.83
COPR5-038-NA	27,248	14	86	3815	23,433	49.73
COPR6-038-A	27,134	1	99	271	26,863	96.42
COPR7-010-NA	27,190	8	92	2175	25,015	71.33
COPR8-010-A	26,925	1	99	269	26,656	96.45

3.3. *Reduction of Cr(VI) in COPR*

The treatment pH, alkaline digestion Cr(VI) concentrations, TCLP Cr and TCLP pH for all the samples are presented in Table 3. The treatment pH of all the samples is less than 9 after a mixing period of 1 h. This pH favors the dissolution of all Cr(VI)-bound minerals and swell-causing minerals. The Cr(VI) concentration as measured by alkaline digestion was less than 2 mg/kg for all these samples, indicating a satisfactory treatment performance. However, when subjected to XANES analyses Cr(VI) concentrations were much greater than those measured by alkaline digestion. The TCLP Cr concentration for the acid pretreated samples (COPR2-150-A, COPR4-075-A, COPR6-038-A, COPR8-010-A) decreased significantly when compared to the non-acid pretreated samples (COPR1-150-NA, COPR3-075-NA, COPR5-038-NA, COPR7-010-NA). For example, for the sample with particle size less than 0.075 mm, the TCLP Cr concentration for the acid pretreated COPR was 1.52 mg/L (COPR4-075-A), whereas, the TCLP Cr concentration for the non-acid pretreated COPR sample was 10.65 mg/L (COPR3-075-NA). The TCLP Cr concentrations of the acid pretreated samples approached the universal treatment standard of 0.6 mg/L but only the sample with particle size less than 0.010 mm (COPR8-010-A) met the above standard.

3.4. *XANES results*

The Cr(VI) concentrations for all the treated samples were measured by XANES. The XANES patterns are presented in Fig. 3 and associated Cr(VI) percentages are shown in Table 4. The percent reduction of Cr(VI) was calculated using the untreated COPR Cr(VI) concentration of 7588 mg/kg as reported previously by Wazne et al. using XANES [14]. For all the particle sizes, the percent reduction of Cr(VI) is greater for the acid pretreated samples than for the non-acid pretreated samples. The percent reduction of Cr(VI) increased for the acid pretreated samples and for the smaller particle size. For example, the Cr(VI) concentrations for the coarse particle size (<0.150 mm) and acid pretreated COPR is 1057 mg/kg, whereas, for the same particle size and non-acid pretreated COPR, the value is 5769 mg/kg. Similarly, for the finest particle size (<0.010 mm), the measured Cr(VI) concentration for the acid pretreated COPR was 269 mg/kg whereas the measured Cr(VI) concentration was 2175 mg/kg for the non-acid pretreated COPR sample. This indicated that approximately 71% Cr(VI) reduction was attained only based on the particle size reduction to 0.01 mm. Moreover, 80% Cr(VI) reduction was further achieved based on the acid addition with particle size of 0.15 mm. The measured concentration of Cr(VI) for the coarsest particle size with acid pre-treatment was 1057 mg/kg, whereas the measured Cr(VI) concentration was 2157 mg/kg for the finest particle size with no acid pre-treatment. This may suggest that the acid dosage is a more important factor in reducing the concentration of Cr(VI) than the particle size reduction. However, without particle size reduction, the best treatment results achieved only partial reduction with residual Cr(VI) concentration of 1057 mg/kg. A maximum Cr(VI) reduction of 96.45% was achieved for the acid pretreated COPR with the lowest particle size of less than 0.010 mm, which corresponds to a Cr(VI) concentration of 269 mg/kg.

For all the samples, the Cr(VI) concentrations as measured by XANES were higher than those obtained by alkaline digestion, which confirms that the alkaline digestion process underestimates Cr(VI) concentrations of Fe(II) treated samples. Similar observations

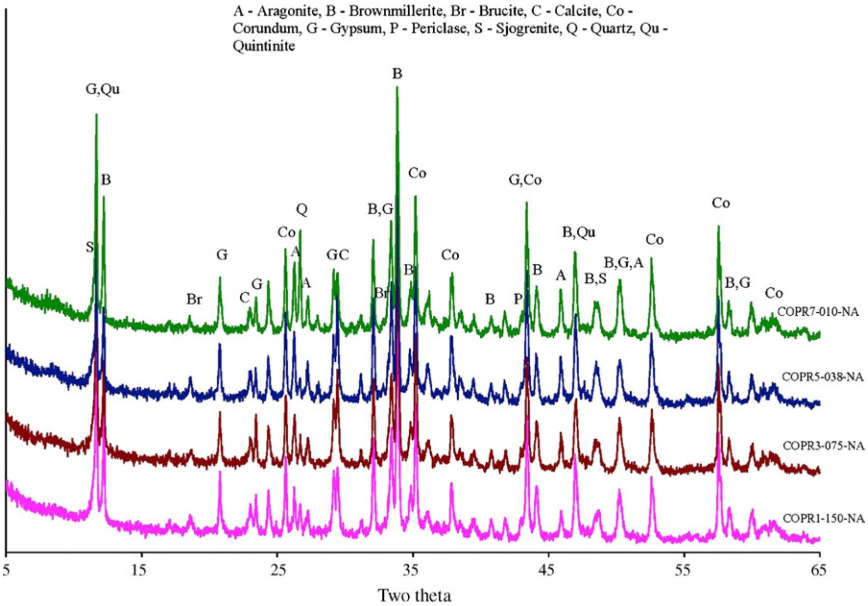

Fig. 4. XRPD patterns for non-acid pretreated samples.

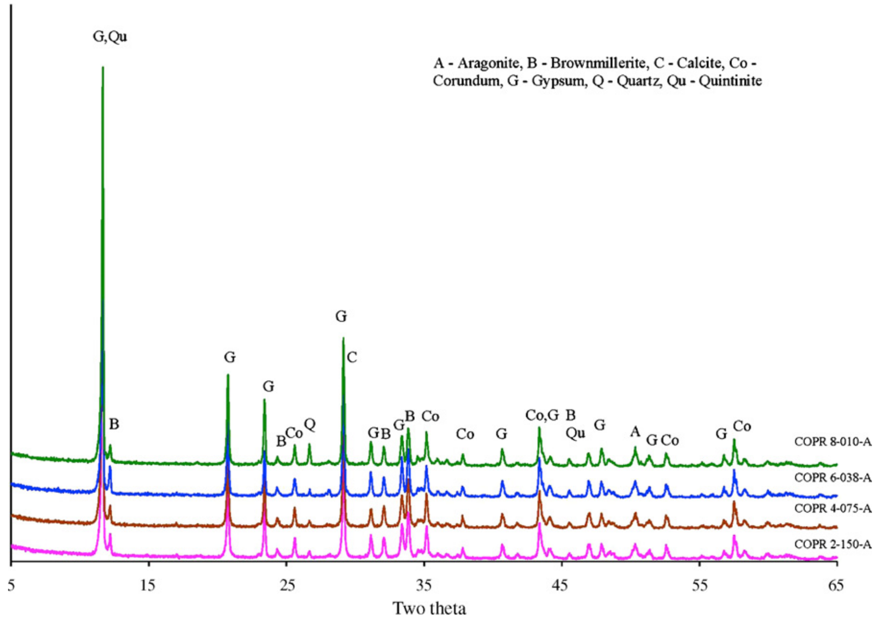

Fig. 5. XRPD patterns for acid pretreated samples.

Table 5
Quantitative results of treated COPR samples.

Mineral name	COPR1-150-NA	COPR2-150-A	COPR3-075-NA	COPR4-075-A	COPR5-038-NA	COPR6-038-A	COPR7-010-NA	COPR8-010-A
Aragonite, $CaCO_3$	5.34	–	9.52	–	11.37	–	11.06	–
Brownmillerite, $Ca_2(Al, Fe^{3+})_2O_5$	22.41	18.73	22.43	19.38	19.28	17.12	20.74	13.75
Calcite, $CaCO_3$	5.10	2.61	7.18	2.38	6.82	8.13	4.68	1.98
Gypsum, $CaSO_4{\cdot}2H_2O$	6.53	33.52	5.88	33.99	6.15	33.84	6.02	38.96
Periclase, MgO	0.52	–	0.20	–	–	–	–	–
Quartz, SiO_2	1.81	1.52	1.69	1.25	1.29	1.44	4.27	3.71
Quintinite, 2H, $Mg_4Al_2(OH)_{12}(CO_3){\cdot}3H_2O$	2.67	2.18	1.45	3.26	3.57	2.56	2.98	3.39
Sjogrenite, $Mg_6Fe^{2+}{}_2CO_3(OH)_{16}{\cdot}4H_2O$	1.62	2.00	–	2.45	1.29	2.49	0.77	2.24
Brucite, $Mg(OH)_2$	1.67	–	1.50	–	1.91	–	0.87	–
Amorphous	52.33	39.38	50.15	37.28	48.31	34.42	48.55	36.03
Total	100.00	99.94	100.00	100.00	100.00	100.00	99.95	100.06

Note: All the values are in percentages.

were also reported for ferrous sulfate treated COPR by Dermatas et al. [7] and Moon et al. [11] and also for calcium polysulfide treated COPR by Wazne et al. [9] and Moon et al. [19].

3.5. XRPD results

The XRPD patterns for the treated COPR samples with acid pretreatment and with no acid pretreatment are presented in Figs. 4 and 5, respectively. The quantitative XRPD results for all treated COPR samples are presented in Table 5. There was a significant change in the mineralogy of the treated COPR. Cr(VI)-hydrocalumite was not observed in any of the treated samples as pH was below its stability regime. Conversely, brownmillerite content decreased for all treated COPR samples. However, a significant decrease (31.2–14%) was observed for the acid pretreated samples with a particle size less than 0.01 mm. This indicates that reduction of particle size and acid addition mitigates the mass transfer limitation hindering brownmillerite hydration. No ettringite peaks were observed for all treated samples, confirming other results [7] indicating that ettringite is not stable in ferrous sulfate treated COPR at pH less than 9 [10]. On the other hand, gypsum peaks are clearly identified for all treated samples. The quantity of gypsum was greater for the acid pretreated COPR samples than for the non-acid pretreated COPR, indicating that acid addition favors gypsum formation. However, gypsum may transform to ettringite in the presence of alumina and alkalinity ($pH > 9$), both of which become available upon hydration of residual brownmillerite. Therefore, residual brownmillerite may play a detrimental role in any treatment scheme if not significantly destabilized. Longer mixing times and more aggressive mixing can be utilized to destabilize residual brownmillerite. More mixing options should become available for future pilot scale programs. Also, addition of soils, which have some buffering capacity, to the treated COPR can be tested (as a polishing step) to neutralize the alkalinity bound in residual brownmillerite if needed.

4. Conclusions

A bench-scale treatability study was performed to evaluate the effects of particle size and acid addition on the remediation of COPR using ferrous sulfate. The acid dosage required to destabilize Cr(VI)-bearing minerals and inhibit ettringite formation as predicted by EQ3/6 was 13 eq $[H^+]$/kg, much greater than 5.5 eq $[H^+]$/kg, calculated from the batch leaching tests after a mixing period of 2 months. This indicated that the system has not reached equilibrium even after 2 months mixing. Also, mass transfer limitation is playing a significant role in impeding the dissolution of COPR minerals and hence the remediation of COPR. Regardless of acid addition and particle size reduction, the TCLP results showed that all treated COPR samples failed to meet the UTS of 0.6 mg/L, except for the acid pretreated sample with particle size less than 0.010 mm. Cr(VI) concentrations for all the treated samples as measured by alkaline digestion were less than the current NJDEP standard of 20 mg/kg. However, the Cr(VI) concentrations as quantified by XANES resulted in higher concentrations than those quantified by alkaline digestion. The lowest Cr(VI) concentration was 269 mg/kg for the acid pretreated sample with particle size less than 0.010 mm. According to XANES results, greater Cr(VI) percentages were reduced with acid pretreatment and particle size reduction. Ettringite was not observed in all treated COPR samples as the treatment pH of all the samples was less than 9.

Acknowledgement

The authors thank the members of the Pohang Accelerator Laboratory (PAL), South Korea for their integral help with XANES analyses.

References

[1] Allied Signal, Process description-Baltimore works, 1982.
[2] R.G. Darrie, Commercial extraction technology and process waste disposal in the manufacture of chromium chemicals from ore, Environ. Geochem. Health 23 (2001) 187–193.
[3] J.S. Geelhoed, J.C.L. Meeussen, S. Hillier, D.G. Lumsdon, R.P. Thomas, Identification and geochemical modeling of processes controlling leaching of Cr(VI) and other major elements from chromite ore processing residue, Geochim. Cosomchim. Acta 66 (2002) 3927–3942.
[4] M. Wazne, S.C. Jagupilla, D.H. Moon, C. Christodoulatos, M. Kaouris, J. Morris, A. Koutsospyros, Leaching mechanisms of Cr(VI) from chromite ore processing residue, J. Environ. Qual. 37 (2008) 2125–2134.
[5] T. Burke, J. Fagliano, M. Goldoft, R.E. Hazen, R. Iglewicz, T. McKee, Chromite ore processing residue in Hudson County, New Jersey, Environ. Health Perspect. 92 (1991) 131–137.
[6] D. Dermatas, R. Bonaparte, M. Chrysochoou, D.H. Moon, Chromite ore processing residue (COPR): contaminated soil or hazardous waste? J. ASTM Int. 3 (7) (2006), doi:10.1520/JAI13313.
[7] D. Dermatas, M. Chrysochoou, D.H. Moon, M. Wazne, C. Christodoulatos, D.G. Grubb, Ettringite induced heave in chromite ore processing residue (COPR) upon ferrous sulfate treatment, Environ. Sci. Technol. 40 (2006) 5786–5792.
[8] D.H. Moon, D. Dermatas, M. Chrysochoou, G. Shen, An investigation of the heaving mechanism related to chromite ore processing residue, J. ASTM Int. 3 (6) (2006), doi:10.1520/JAI13309.
[9] M. Wazne, S.C. Jagupilla, D.H. Moon, S.C. Jagupilla, C. Christodoulatos, M.G. Kim, Assessment of calcium polysulfide for the remediation of hexavalent chromium in chromite ore processing residue (COPR), J. Hazard. Mater. 143 (2007) 620–628.
[10] M. Wazne, D.H. Moon, S.C. Jagupilla, S.C. Jagupilla, C. Christodoulatos, D. Dermatas, M. Chrysochoou, Remediation of chromite ore processing residue using ferrous sulfate and calcium polysulfide, Geosci. J. 11 (2007) 105–110.
[11] D.H. Moon, M. Wazne, D. Dermatas, C. Christodoulatos, A.M. Sanchez, D.G. Grubb, M. Chrysochoou, M.G. Kim, Long-term treatment issues with chromite ore processing residue (COPR): Cr^{6+} reduction and heave, J. Hazard. Mater. 143 (2007) 629–635.
[12] D.F. Tamas, A. Vertes, A Mossbauer study of the hydration of brownmillerite, Cement Concrete Res. 3 (1972) 575–581.
[13] D.D. Kremser, B.M. Sass, G.I. Clark, M. Bhargava, C. French, Environmental forensics investigation of buried chromite ore processing residue, in: Proceedings of the 8th International In Situ and On-Site Bioremediation Symposium, Baltimore, Maryland, USA, June 6–9, 2005.
[14] S. Hillier, M.J. Roe, J.S. Geelhoed, A.R. Fraser, J.G. Farmer, E. Paterson, Role of quantitative mineralogical analysis in the investigation of sites contaminated by chromite ore processing residue, Sci. Total Environ. 308 (2003) 195–210.
[15] T.L. Rinehart, D.G. Schulze, R.M. Bricka, S. Bajt, E.R. Blatchley, Chromium leaching vs. oxidation state for a contaminated solidified/stabilized soil, J. Hazard. Mater. 52 (1997) 213–221.
[16] L.L. Eary, D. Rai, Chromate removal from aqueous wastes by reduction with ferrous iron, Environ. Sci. Technol. 22 (8) (1988) 676–683.
[17] J.S. Geelhoed, J.C.N. Meeussen, M.J. Roe, S. Hiller, R.P. Thomas, J.G. Farmer, E. Paterson, Chromium remediation or release? Effect of iron(II) sulfate addition on chromium(VI) leaching from columns of chromite ore processing residue, Environ. Sci. Technol. 37 (14) (2003) 3206–3213.
[18] M.C. Graham, J.G. Farmer, P. Anderson, E. Paterson, S. Hillier, D.G. Lumsdon, R. Bewley, Calcium polysulfide remediation of hexavalent chromium contamination from chromite ore processing residue, Sci. Total Environ. 364 (2006) 32–44.
[19] D.H. Moon, M. Wazne, S.C. Jagupilla, C. Christodoulatos, M.G. Kim, A. Koutsospyros, Particle size and pH effects on remediation of chromite ore processing residue using calcium polysulfide (CaS_5), Sci. Total Environ. 399 (2008) 2–10.
[20] C. Su, R.D. Ludwig, Treatment of hexavalent chromium in chromite ore processing solid waste using a mixed reductant solution of ferrous sulfate and sodium dithionite, Environ. Sci. Technol. 39 (2005) 6208–6216.
[21] S. Hillier, D.G. Lumsdon, R. Brydson, E. Paterson, Hydrogarnet: a host phase for Cr(VI) in chromite ore processing residue (COPR) and other high pH wastes, Environ. Sci. Technol. 41 (2007) 1921–1927.
[22] J.M. Tinjum, C.H. Benson, T.B. Edil, Mobilization of Cr(VI) from chromite ore processing residue through acid treatment, Sci. Total Environ. 391 (1) (2008) 13–25.
[23] J. Isenburg, M. Moore, Generalized acid neutralization capacity test, in: T.M. Gilliam, C.C. Wiles (Eds.), Stabilization and Solidification of Hazardous, Radioactive, and Mixed Wastes, ASTM STP 1123, vol. 2, American Society for Testing and Materials, Philadelphia, 1992, pp. 361–377.
[24] T.J. Wolery, EQ3NR, A computer program for geochemical aqueous speciation-solubility calculations: theoretical manual, user's guide and related documentation (version 7.0), Report UCRL-MA-110662 PT III, Lawrence Livermore National Laboratory, Livermore, 1992.
[25] T. Wolery, S.A. Daveler, EQ6, A computer program for reaction path modeling of aqueous geochemical systems: theoretical manual, user's guide, and related documentation (version 7.0), Report UCRL-MA-110662 PT IV, Lawrence Livermore National Laboratory, Livermore, 1992.
[26] A.F. Gualtieri, P. Venturelli, In situ study of the goethite-hematite phase transformation by real time synchrotron powder diffraction, Am. Miner. 84 (1999) 895–904.
[27] ASTM International, D4972-01, Standard test method for pH of soils.
[28] U.S. Environmental Protection Agency, Microwave assisted acid digestion of sediments, sludges, soils and oils, Method 3051A, Washington, DC, 2007.
[29] U.S. Environmental Protection Agency, Inductively coupled plasma–atomic emission spectroscopy, Method 6010C, Washington, DC, 2007.
[30] U.S. Environmental Protection Agency, Alkaline digestion for hexavalent chromium, Method 3060A, Washington, DC, 1996.
[31] U.S. Environmental Protection Agency, Chromium, hexavalent (colorimetric), Method 7196A, Washington, DC, 1992.
[32] U.S. Environmental Protection Agency, Toxicity Characteristic Leaching Procedure, Method 1311, Washington, DC, 1992.
[33] Materials Data Inc., Jade Version 7.5, California, USA, 2006.
[34] H.M. Rietveld, A profile refinement method for nuclear and magnetic structures, J. Appl. Crystallogr. 2 (1969) 65–71.
[35] International Centre for Diffraction Data (ICDD), Powder Diffraction File, PDF-2 Database Release, 2004.
[36] Inorganic Crystal Structure Database (ICSD), Germany, 2007.
[37] M. Newville, IFEFFIT: interactive XAFS analysis and FEFF fitting, J. Synchrotron Radiat. 8 (2001) 322–324.